Kaon-meson condensation and Δ resonance in hyperonic stellar matter within a relativistic mean-field model

Fu Ma,[1] Chen Wu,[2,*] and Wenjun Guo[1]
[1]*University of Shanghai for Science and Technology, Shanghai 200093, China*
[2]*Shanghai Advanced Research Institute, Chinese Academy of Sciences, Shanghai 201210, China*

(Received 15 November 2022; accepted 3 April 2023; published 13 April 2023)

We study the equation of state of dense baryon matter within the relativistic mean-field model, and we include $\Delta(1232)$ isobars in the Indiana University–Florida State University (IUFSU) model with hyperons and consider the possibility of kaon meson condensation. We find that it is necessary to consider the Δ resonance state inside a massive neutron star. The critical density of kaon mesons and hyperons is shifted to a higher density region; in this respect an early appearance of Δ resonances is crucial to guarantee the stability of the branch of hyperonized star with the difference of the coupling parameter $x_{\sigma\Delta}$ constrained based on the QCD rules in nuclear matter. The Δ resonance produces a softer equation of state in the low density region, which makes the tidal deformability and radius consistent with the observation of GW170817. As the addition of new degrees of freedom will lead to a softening of the equation of state, the σ-cut scheme, which states that the decrease of neutron star mass can be lowered if one assumes a limited decrease of the σ-meson strength at ρ_B ($\rho_B > \rho_0$), finally we get a maximum mass neutron star with Δ resonance heavier than $2M_\odot$.

DOI: 10.1103/PhysRevC.107.045804

I. INTRODUCTION

Astronomical observations and gravitational wave data over the past decade have placed a series of constraints on a range of properties of neutron stars (mass, radius, deformabilities, for example). The massive neutron stars (NSs) observed, e.g., PSR J1614−2230 with $M = 1.908 \pm 0.016\,M_\odot$ [1–4], have established strong constraints on the equation of state (EOS) of nuclear matter. PSR J0348+0432 with $M = 2.01 \pm 0.04M_\odot$ [5], MSP J0740+6620 with $M = 2.08^{+0.07}_{-0.07}M_\odot$ [6,7], and radius $12.39^{+1.30}_{-0.98}$ km obtained from NICER data [8]. The recent observation of gravitational waves from the binary neutron star merger event GW170817 suggests that the dimensionless combined tidal deformability Λ is considered to be less than 720 at 90% confidence level based on low spin priors [9], while a lower limit with $\Lambda \geqslant 197$ is obtained based on electromagnetic observations of the transient counterpart AT2017gfo [10]. These astronomical observations constrain the tidal deformability of a $1.4M_\odot$ mass neutron star and thus strong interactions in dense nuclear matter. These upper limits indicate that the EOS of stellar material is softened at this (intermediate) density. One way to solve this problem is to introduce new degrees of freedom (hyperons [11,12], Δ resonance [13–21], kaon meson condensation [22–26]); as the density of nucleons increases, the appearance of hyperons, Δ resonance, and kaon condensation inevitably softens the equation of state, resulting in a neutron star with a mass and radius consistent with astronomical observations.

As the density of nucleons increases, hadron degrees of freedom inside the neutron star are excited into strangeness-bearing hyperons; they affect the stellar structure and evolution in various ways [27,28]. Although the existence of hyperons inside neutron stars is inevitable, their appearance will significantly lead to a softening of the equation of state, resulting in a decrease in the maximum mass of the neutron star, which does not correspond to the observation of massive neutron stars ($2M_\odot$); this is known as the hyperon puzzle [29–31]. In order to guarantee a stiffer EOS and massive neutron stars, density covariant functional theory has been chosen to study neutron stars containing hyperons [17,32–36,36,37]. However, with the constraints on tidal deformation and radii imposed by astronomical observations, the application of this theoretical model is subject to some limitations [38,39].

Although there are many speculations about the existence of hyperons inside neutron stars, there is little discussion about the Δ resonance. One reason is that early work suggested that the critical densities of Δ resonances in the relativistic mean-field (RMF) model with the same strength of the meson field as the nucleon case exceed the densities of the core of typical neutron stars [18,40], which is considered out of the realm of astrophysics. Another reason is that the occurrence of Δ resonance leads to a softening of the equation of state, which has become a Δ puzzle [17] in some literature, the same as the hyperon puzzle. However, recent work has shown that considering the Δ resonance inside a neutron star reduces the radius of a NS with a standard mass of $1.4M_\odot$, and that the equation of state does not change significantly [37,41,42].

Another new degree of freedom for non-nucleons in dense stars includes various meson (kaon, pion) condensates [43,44]. Kaplan and Nelson have suggested that the ground state of hadronic matter might form a negatively charged kaon Bose-Einstein condensation above a certain critical density

*wuchenoffd@gmail.com

[45,46]. In the interior of a neutron star, as the density of neutrons increases, the electronic chemical potential will increase to keep the matter in β equilibrium. When the electronic chemical potential exceeds the mass of muons, muons appear. And when the vacuum mass of the meson (pion, kaon) is exceeded, as the density increases, negatively charged mesons begin to appear, which helps to maintain electrical neutrality. However, the s-wave πN scattering potential repels the ground state mass of the π meson and prevents the generation of the π meson [18]. With the increase of density, the energy ω_K of a test kaon in the pure normal phase can be computed as a function of the nucleon density. The kaon energy will decrease while the chemical potential of the kaon increases with the density. When the condition $\omega_K = \mu_e$ is achieved, the kaon will occupy a small fraction of the total volume, then K^- will be more advantageous than electrons as a neutralizer for positive charges, and this will open the possibility of the appearance of kaon condensates.

Many scholars have proposed various density covariant functional theories or realistic nuclear potentials in order to obtain more massive neutron stars containing hyperons. However these theories are usually used to consider neutrons, protons, and leptons (n, p, e, μ^-) because of the hyperon puzzle, and considering hyperons in the RMF framework leads to a reduction of the maximum mass of neutron stars and thus does not satisfy astronomical observations. However, the σ-cut scheme [47] points out that, in the small scale range where the density $\rho_B > \rho_0$, a sharp decrease in the strength of the σ meson reduces the decrease in the effective mass of the nucleon, which eventually stiffens the EOS and still yields neutron stars of more than $2M_\odot$ after considering the hyperon degrees of freedom [48,49]. In this article, we use the Indiana University–Florida State University (IUFSU) model [50,51] to study NS matter including hyperons, Δ resonance, and kaon condensates with the σ-cut scheme.

This paper is organized as follows. First, the theoretical framework is presented. Then we will study the effects of kaon meson condensation and Δ resonance containing hyperons with the σ-cut scheme. Finally, some conclusions are provided.

II. THEORETICAL FRAMEWORK

In this section, we introduce the IUFSU model to study the properties of the Δ resonance and phase transition from hadronic to kaon condensed matter. For the baryon matter we have considered nucleons (n and p), hyperons (Λ, Σ, and Ξ), Δ resonances (Δ^{++}, Δ^+, Δ^0, Δ^-), and kaons (K^-). The exchanged mesons include the isoscalar scalar meson (σ), the isoscalar vector meson (ω), the isovector vector meson (ρ), and the strange vector meson (ϕ). The starting point of the extended IUFSU model is the Lagrangian density:

$$
\begin{aligned}
\mathcal{L} = &\sum_B \bar{\psi}_B[i\gamma^\mu\partial\mu - m_B + g_{\sigma B}\sigma - g_{\omega B}\gamma^\mu\omega_\mu - g_{\phi B}\gamma^\mu\phi_\mu - g_{\rho B}\gamma^\mu\vec{\tau}\cdot\vec{\rho^\mu}]\psi_B \\
&+ \sum_D \bar{\psi}_D[i\gamma^\mu\partial\mu - m_D + g_{\sigma D}\sigma - g_{\omega D}\gamma^\mu\omega_\mu - g_{\phi D}\gamma^\mu\phi_\mu - g_{\rho D}\gamma^\mu\vec{\tau}\cdot\vec{\rho^\mu}]\psi_D \\
&+ \frac{1}{2}\partial_\mu\sigma\partial^\mu\sigma - \frac{1}{2}m_\sigma^2\sigma^2 - \frac{\kappa}{3!}(g_{\sigma N}\sigma)^3 - \frac{\lambda}{4!}(g_{\sigma N}\sigma)^4 - \frac{1}{4}F_{\mu\nu}F^{\mu\nu} + \frac{1}{2}m_\omega^2\omega_\mu\omega^\mu - \frac{1}{4}\Phi_{\mu\nu}\Phi^{\mu\nu} \\
&+ \frac{1}{2}m_\phi^2\phi_\mu\phi^\mu + \frac{\xi}{4!}\left(g_{\omega N}^2\omega_\mu\omega^\mu\right)^2 + \frac{1}{2}m_\rho^2\vec{\rho}_\mu\cdot\vec{\rho}^\mu - \frac{1}{4}\vec{G}_{\mu\nu}\vec{G}^{\mu\nu} + \Lambda_\nu\left(g_{\rho N}^2\vec{\rho}_\mu\cdot\vec{\rho}^\mu\right)\left(g_{\omega N}^2\omega_\mu\omega^\mu\right) \\
&+ \sum_l \bar{\psi}_l[i\gamma^\mu\partial\mu - m_l]\psi_l,
\end{aligned}
\tag{1}
$$

with the field tensors

$$
\begin{aligned}
F_{\mu\nu} &= \partial_\mu\omega_\nu - \partial_\nu\omega_\mu, \\
\Phi_{\mu\nu} &= \partial_\mu\phi_\nu - \partial_\nu\phi_\mu, \\
\vec{G}_{\mu\nu} &= \partial_\mu\rho_\nu - \partial_\nu\rho_\mu.
\end{aligned}
\tag{2}
$$

The model contains following quantities: the baryon octet and two leptons $(p, n, e, \mu, \Lambda^0, \Sigma^+, \Sigma^0, \Sigma^-, \Xi^0, \Xi^-)$, Δ resonances (Δ^{++}, Δ^+, Δ^0, Δ^-), isoscalar-scalar σ, isoscalar-vector ω, ϕ, and isoscalar-vector ρ with the masses and coupling constants. The isospin operator for the isovector-vector meson fields is represented by $\vec{\tau}$, where Λ_ν is introduced to modify the density dependence of symmetry energy. The isoscalar meson self-interactions (via κ, λ, and ξ terms) are necessary for the appropriate EOS of symmetric nuclear matter. In RMF models, the operators of meson fields are replaced by their expectation values using the mean-field approximation. In Table I, we list properties and coupling constants for baryons other than nucleons in Eq. (1).

We take the Lagrangian of kaon condensation as the same that in Refs. [43] and [44], which reads

$$
\mathcal{L}_K = D_\mu^* K^* D^\mu K - m_K^{*2} K^* K,
\tag{3}
$$

where $D_\mu = \partial_\mu + ig_{\omega K}\omega_\mu + ig_{\phi K}\phi + i\frac{g_{\rho K}}{2}\tau_K\cdot\rho_\mu$ is the covariant derivative and the kaon effective mass is defined as $m_K^* = m_K - g_{\sigma K}\sigma$.

Finally, with the Euler-Lagrange equation, the equations of motion for baryons and mesons are obtained:

TABLE I. Strangeness mass M, third component of isospin τ_3, charge q, and total angular momentum and parity J^P for Λ^0, $\Sigma^{+,0,-}$, and $\Xi^{-,0}$ hyperons and Δ baryons.

	M (MeV)	τ_3	$q(e)$	J^P
Λ^0	1116	0	0	$(1/2)^+$
Σ^+	1193	1	+1	$(1/2)^+$
Σ^0	1193	0	0	$(1/2)^+$
Σ^-	1193	−1	−1	$(1/2)^+$
Ξ^0	1318	(1/2)	0	$(1/2)^+$
Ξ^-	1318	(−1/2)	−1	$(1/2)^+$
Δ^{++}	1232	(+3/2)	+2	$(3/2)^+$
Δ^+	1232	(+1/2)	+1	$(3/2)^+$
Δ^0	1232	(−1/2)	0	$(3/2)^+$
Δ^-	1232	(−3/2)	−1	$(3/2)^+$

$$
\begin{aligned}
m_\sigma^2\sigma + \frac{1}{2}\kappa g_{\sigma N}^3\sigma^2 + \frac{1}{6}\lambda g_{\sigma N}^4\sigma^3 &= \sum_B g_{\sigma B}\rho_B^S + \sum_D g_{\sigma D}\rho_D^S \\
&\quad + g_{\sigma K}\rho_K,\ m_\omega^2\omega + \frac{\xi}{6}g_{\omega N}^4\omega^3 + 2\Lambda_v g_{\rho N}^2 g_{\omega N}^2\rho^2\omega \\
&= \sum_B g_{\omega B}\rho_B + \sum_D g_{\omega D}\rho_D - g_{\omega K}\rho_K,\ m_\rho^2\rho + 2\Lambda_v g_{\rho N}^2 g_{\omega N}^2\omega^2\rho \\
&= \sum_B g_{\rho B}\tau_{3B}\rho_B + \sum_D g_{\rho D}\tau_{3D}\rho_D - \frac{g_{\rho K}}{2}\rho_K,\ m_\phi^2\phi \\
&= \sum_B g_{\phi B}\rho_B - g_{\phi K}\rho_K,
\end{aligned}
\tag{4}
$$

where $\rho_{B(D)}$ and $\rho_{B(D)}^S$ are the baryon (Δ) density and the scalar density, which read

$$
\begin{aligned}
\rho_B &= \frac{\gamma k_{fB}}{6\pi^2}, \\
\rho_B^S &= \frac{\gamma M^*}{4\pi^2}\left[k_{fB}E_{fB}^* - M^{*2}\ln\left(\frac{k_{fB}+E_{fB}^*}{M^{*2}}\right)\right].
\end{aligned}
\tag{5}
$$

$\gamma = 2$ for baryons and $\gamma = 4$ for Δ resonance. Here $E_{fB}^* = \sqrt{k_{fB}^2 + M^{*2}}$. the kaon density

$$
\rho_K = 2\Big(\omega_K + g_{\omega K}\omega + g_{\phi K}\phi + \frac{g_{\rho K}}{2}\rho\Big)K^*K, \tag{6}
$$

Now, we are in a position to discuss the coupling parameters between baryons (nucleons, hyperons, and Δ) or K^- and meson fields. The masses of nucleons and mesons and the coupling constants between nucleons and mesons in IUFSU models are tabulated in Table II.

For the meson-hyperon couplings, we take those in the SU(6) symmetry for the vector couplings constants:

$$
\begin{aligned}
g_{\rho\Lambda} &= 0,\ g_{\rho\Sigma} = 2g_{\rho\Xi} = 2g_{\rho N}, \\
g_{\omega\Lambda} &= g_{\omega\Sigma} = 2g_{\omega\Xi} = \frac{2}{3}g_{\omega N}, \\
2g_{\phi\Lambda} &= 2g_{\phi\Sigma} = g_{\phi\Xi} = \frac{-2\sqrt{2}}{3}g_{\omega N}.
\end{aligned}
\tag{7}
$$

TABLE III. scalar meson hyperon coupling constants for IUFSU.

	Λ	Σ	Ξ
$x_{\sigma Y}$	0.615 796	0.452 19	0.305 171

The nucleons do not couple to the strange mesons, $g_{\phi N} = 0$, and the mass of meson ϕ takes $M_\phi = 1020$ MeV. The scalar couplings are usually fixed by fitting hyperon potentials with $U_Y^{(N)} = g_{\omega Y}\omega_0 - g_{\sigma Y}\sigma_0$, where σ_0 and ω_0 are the values of the scalar and vector meson strengths at saturation density [52]. We choose the hyperon-nucleon potentials of Λ, Σ, and Ξ as $U_\Lambda^N = -30$ MeV, $U_\Sigma^N = 30$ MeV, and $U_\Xi^N = -18$ MeV [53–55]. Table III provides the numerical values of the meson hyperon couplings at nuclear saturation density, where $x_{\sigma Y} = g_{\sigma Y}/g_{\sigma N}$

The coupling constants between the vector meson and the kaon, $g_{\omega K}, g_{\rho K}$, are determined by the meson SU(3) symmetry as $g_{\omega K} = g_{\omega N}/3$, $g_{\rho K} = g_{\rho N}$ [26], and $g_{\phi K} = 4.27$ for the ϕ meson [56]. The scalar coupling constant $g_{\sigma K}$ is fixed to the optical potential of the K^- in saturated nuclear matter,

$$
U_K(\rho_0) = -g_{\sigma K}\sigma(\rho_0) - g_{\omega K}\omega(\rho_0), \tag{8}
$$

and in this paper we carry out our calculations with a series of optical potentials ranging from −160 to −120 MeV. The $g_{\sigma K}$ can be related to the potential of thekaon at the saturated density through Eq. (8). $g_{\sigma K}$ values corresponding to several values of U_K are listed in Table IV.

Because experimental data on the Δ resonance are scarce, the coupling parameters between the Δ resonances and meson fields are uncertain, so we limit ourselves to considering only the couplings with σ meson fields, which are explored in the literature [57,58]. We assume the scalar coupling ratio $x_{\sigma\Delta} = g_{\sigma\Delta}/g_{\sigma N} > 1$ with a value close to the mass ratio of the Δ and the nucleon [59], and adopt three different choices ($x_{\sigma\Delta} = 1.05$, $x_{\sigma\Delta} = 1.1$, and $x_{\sigma\Delta} = 1.15$) [60]; for $x_{\omega\Delta}$ and $x_{\rho\Delta}$ we take $x_{\omega\Delta} = g_{\omega\Delta}/g_{\omega N} = 1.1$ and $x_{\rho\Delta} = g_{\rho\Delta}/g_{\rho N} = 1$ [61]. Similarly to the nucleons, Δ resonances do not couple to meson ϕ, so $g_{\phi\Delta} = 0$.

By solving the Euler-Lagrangian equation of the kaon we obtain the equation of motion: $[D_\mu D^\mu + m_K^{*2}]K = 0$. We can then derive the dispersion relation for the Bose condensation of K^-, which reads

$$
\omega_K = m_K - g_{\sigma K}\sigma - g_{\omega K}\omega - g_{\phi K}\phi - \frac{g_{\rho K}}{2}\rho. \tag{9}
$$

TABLE II. Parameter sets for the IUFSU model discussed in the text and the meson masses $M_\sigma = 491.5$ (MeV), $M_\omega = 786$ MeV, $M_\rho = 763$ MeV.

Model	g_σ	g_ω	g_ρ	κ	λ	ξ	Λ_v
IUFSU	9.9713	13.0321	13.5899	3.376 85	0.000 268	0.03	0.046

TABLE IV. $g_{\sigma K}$ determined for several U_K values in the IUFSU model.

U_K (MeV)	−120	−140	−160
$g_{\sigma K}$	0.600 417	1.144 204	1.687 99

For the neutron matter with baryons and charged leptons, the β-equilibrium conditions are guaranteed with the following relations of chemical potentials for different particles:

$$\begin{aligned} \mu_p &= \mu_{\Sigma^+} = \mu_{\Delta^+}, \\ \mu_\Lambda &= \mu_{\Sigma^0} = \mu_{\Xi^0} = \mu_{\Delta^0} = \mu_n, \\ \mu_{\Sigma^-} &= \mu_{\Xi^-} = \mu_{\Delta^-} = 2\mu_n - \mu_p, \\ \mu_{\Delta^{++}} &= 2\mu_p - \mu_n, \\ \mu_\mu &= \mu_e = \mu_n - \mu_p, \end{aligned} \tag{10}$$

and the charge neutrality condition is fulfilled by

$$\sum_B q_B\rho_B + \sum_D q_D\rho_D - \rho_K - \rho_e - \rho_\mu = 0. \tag{11}$$

The chemical potentials of baryons, Δ, and leptons read:

$$\mu_i = \sqrt{k_F^{i2} + m_i^{*2}} + g_{\omega i}\omega + g_{\phi i}\phi + g_{\rho i}\tau_{3i}\rho, \quad i = B, D, \tag{12}$$

$$\mu_l = \sqrt{k_F^{l2} + m_l^2}, \tag{13}$$

where k_F^i is the Fermi momentum and m_i^* is the effective mass of baryon and Δ resonances, which can be related to the scalar meson field as $m_i^* = m_i - g_{\sigma i}\sigma$, and k_F^l is the Fermi momentum of the lepton $l(\mu, e)$.

The total energy density of the system with kaon condensation, $\varepsilon = \varepsilon_{(B,D)} + \varepsilon_K$, where $\varepsilon_{B,D}$ is the energy density of baryons and Δ resonances, can be given as

$$\begin{aligned} \varepsilon_{B,D} = &\sum_{i=B,D} \frac{\gamma}{(2\pi)^3}\int_0^{k_{Fi}} \sqrt{m_i^* + k^2}d^3k + \frac{1}{2}m_\omega^2\omega^2 \\ &+ \frac{\xi}{8}g_{\omega N}^4\omega^4 + \frac{1}{2}m_\sigma^2\sigma^2 + \frac{\kappa}{6}g_{\sigma N}^3\sigma^3 + \frac{\lambda}{24}g_{\sigma N}^4\sigma^4 \\ &+ \frac{1}{2}m_\rho^2\rho^2 + 3\Lambda_\nu g_{\rho N}^2 g_{\omega N}^2\omega^2\rho^2 + \frac{1}{2}m_\phi^2\phi^2 \\ &+ \frac{1}{\pi^2}\sum_l \int_0^{k_{Fl}} \sqrt{k^2 + m_l^2}k^2dk, \end{aligned} \tag{14}$$

And the energy contributed by the kaon condensation ε_K is

$$\varepsilon_K = 2m_K^{*2}K^*K = m_K^*\rho_K.. \tag{15}$$

The kaon does not contribute directly to the pressure as it is a (s-wave) Bose condensate, so that the expression of pressure reads

$$P = \sum_{i=B,D} \mu_i\rho_i + \sum_{l=\mu,e} \mu_l\rho_l - \varepsilon. \tag{16}$$

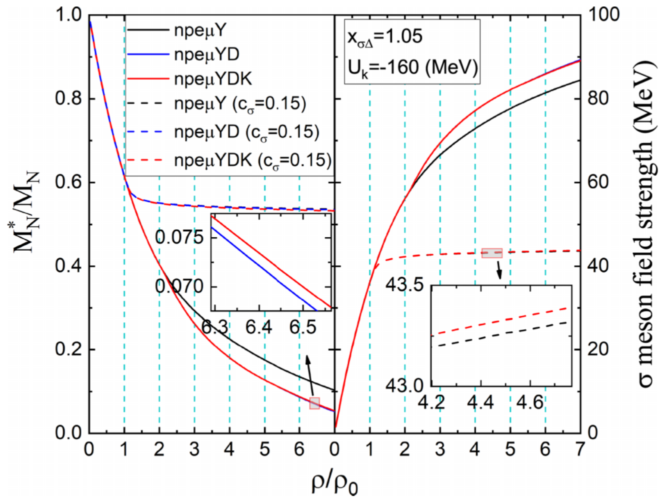

FIG. 1. Effective mass and σ meson strength of nucleons versus baryon density in NS matter using and not using σ-cut scheme.

With the obtained ε and P, the mass-radius relation and other relevant quantities of neutron star can be obtained by solving the Oppenheimer and Volkoff equation [62]:

$$\begin{aligned} \frac{dP(r)}{dr} = &-\frac{GM(r)\varepsilon}{r^2}\left(1 + \frac{P}{\varepsilon C^2}\right)\left(1 + \frac{4\pi r^3 P}{M(r)C^2}\right) \\ &\times \left(1 - \frac{2GM(r)}{rC^2}\right)^{-1}, \end{aligned} \tag{17}$$

$$dM(r) = 4\pi r^2\varepsilon(r)dr. \tag{18}$$

The tidal deformability of a neutron star is reduced as a dimensionless form [63,64],

$$\Lambda = \frac{2}{3}k_2C^{-5}, \tag{19}$$

where $C = GM/R$, and the second Love number k_2 can be fixed simultaneously with the structures of compact stars [65].

The σ-cut scheme [47], which is able to stiffen the EOS above saturation density, adds in the original Lagrangian density the function [47,66,67]

$$\Delta U(\sigma) = \alpha \ln\{1 + \exp[\beta(f - f_{s,core})]\}, \tag{20}$$

where $f = g_{\sigma N}\sigma/M_N$ and $f_{s,core} = f_0 + c_\sigma(1 - f_0)$. M_N is the nucleon mass. f_0 is the value of f at saturation density, equal to 0.31 for the IUFSU model. c_σ is a positive parameter that we can adjust. The smaller c_σ is, the stronger the effect of the σ-cut scheme becomes. However, we must be careful that this scheme would not affect the saturation properties of nuclear matter; in our previous work we discussed in detail the choice of parameter c_σ [48]. In this paper, we take $c_\sigma = 0.15$ to satisfy the maximum mass constraint. α and β are constants, taken to be $4.822 \times 10^{-4}M_N^4$ and 120 as in Ref. [47]. This scheme stiffens the EOS by quenching the decrease of the effective mass of the nucleon $M_N^* = M_N(1 - f)$ at high density.

III. RESULTS

First, we studied the effect of the σ-cut scheme on the IUFSU model. In Fig. 1, we plot the ratio of the effective

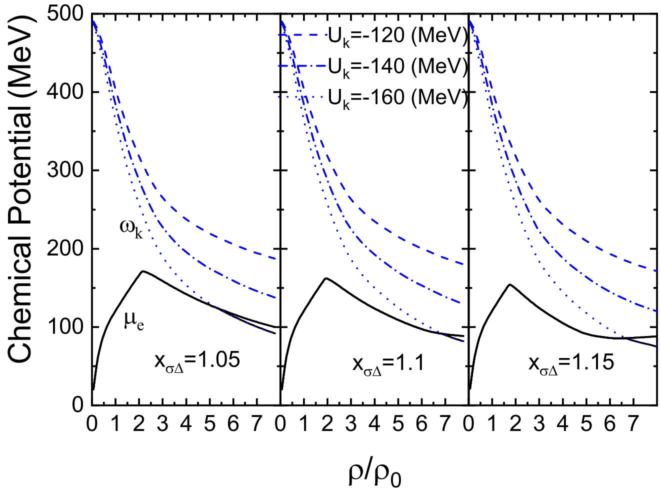

FIG. 2. Kaon meson energy (ω_K) and electronic chemical potential (μ_e) as a function of ρ_B with different $x_{\sigma\Delta}$ and U_K, and without σ-cut scheme.

mass of nucleons to the rest mass and the σ meson strength as a function of the baryon density, where ρ_0 is the saturation density, and we choose $x_{\sigma\Delta} = 1.05$ and $U_K = -160$ MeV to consider Δ resonance and kaon condensation. From the left panel, we can see that when $\rho \leqslant \rho_0$ the effective mass is almost same as nucleons-only matter and is unchanged by the σ-cut scheme; when $\rho > \rho_0$, the effective mass drops to around $0.55M_N$. And it is obviously observed that under the σ-cut scheme considering or not considering Δ and K^- in the EOS has very tiny effect on the effective mass of nucleons. From the right panel, when $\rho > \rho_0$, the σ meson field strength is quenched at high baryon density; this is what we want from using the σ-cut scheme.

In Fig. 2, we plot the chemical potential of K^- and e^- as a function of baryon density. With the increase of density, the energy ω_K of a test kaon in the pure normal phase can be computed as a function of the nucleon density. The

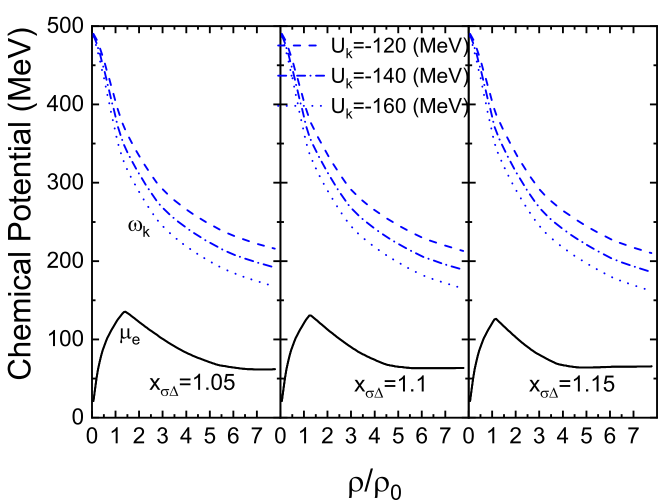

FIG. 3. Kaon energy(ω_k) and electron chemical potential (u_e) as a function of baryon density with different $x_{\sigma\Delta}$ and U_K; $c_\sigma = 0.15$.

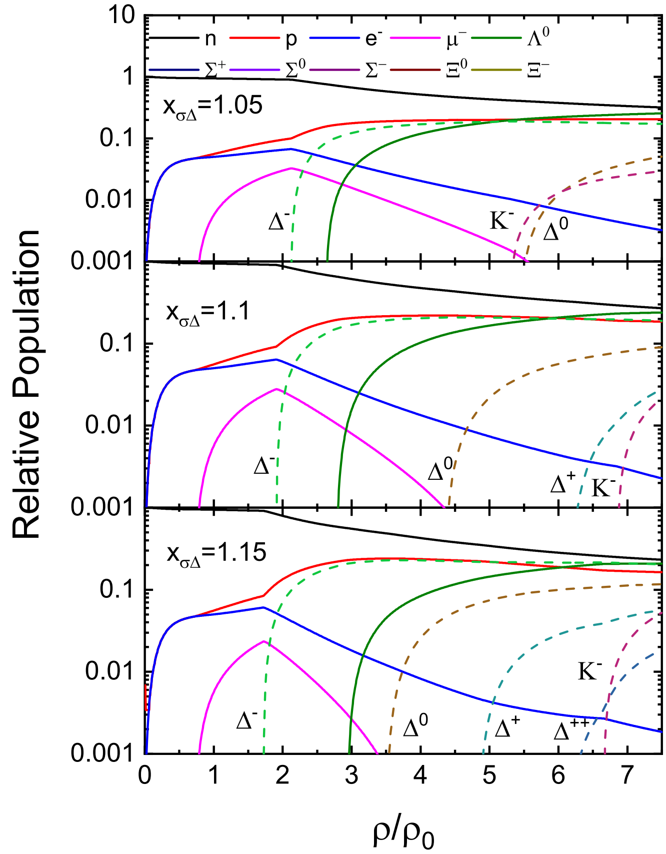

FIG. 4. Relative population of particles versus baryon density without σ-cut scheme with $x_{\sigma\Delta} = 1.05$, $x_{\sigma\Delta} = 1.1$, $x_{\sigma\Delta} = 1.15$, and K^- potential depth of $U_K = -160$ MeV; dashed lines denote K^- and Δ resonance.

kaon energy(ω_K) will decrease while the electron chemical potential (μ_e) increases with the density. When the condition $\omega_K = \mu_e$ is achieved, the kaon will occupy a small fraction of the total volume. We can see that both $x_{\sigma\Delta}$ and U_K affect the kaon meson condensation. From $x_{\sigma\Delta} = 1.05$ to 1.15, there is no intersection between ω_K and μ_e when $U_k = -120$ and -140 MeV. The intersection of ω_K and μ_e is only possible when $U_K = -160$ MeV, which means that the smaller the optical potential of the K^- at saturated nuclear matter is, the greater the possibility of the kaon condensation is. When we choose the σ-cut scheme (Fig. 3), there is no intersection between ω_K and μ_e. The decrease of σ meson field strength slows down the decline of ω_K, and makes the appearance of K^- difficult. We list the threshold densities n_{cr} for kaon condensation for different values of K^- optical potential depths U_K in Table V.

Figure 4 shows the relative population of particles versus baryon density with $x_{\sigma\Delta} = 1.05$, $x_{\sigma\Delta} = 1.1$, $x_{\sigma\Delta} = 1.15$, and $U_K = -160$ MeV. We find that, as $x_{\sigma\Delta}$ increases, the critical density of Λ^0 moves to a higher density region, while the density of leptons moves to a lower density; and in particular as μ^- disappear, Δ^0 start to appear and the critical density of Δ resonance moves to a lower density region. When $x_{\sigma\Delta} = 1.1$, Δ^+ appears at $6.21\rho_0$, and for $x_{\sigma\Delta} = 1.15$, Δ^{++} appears

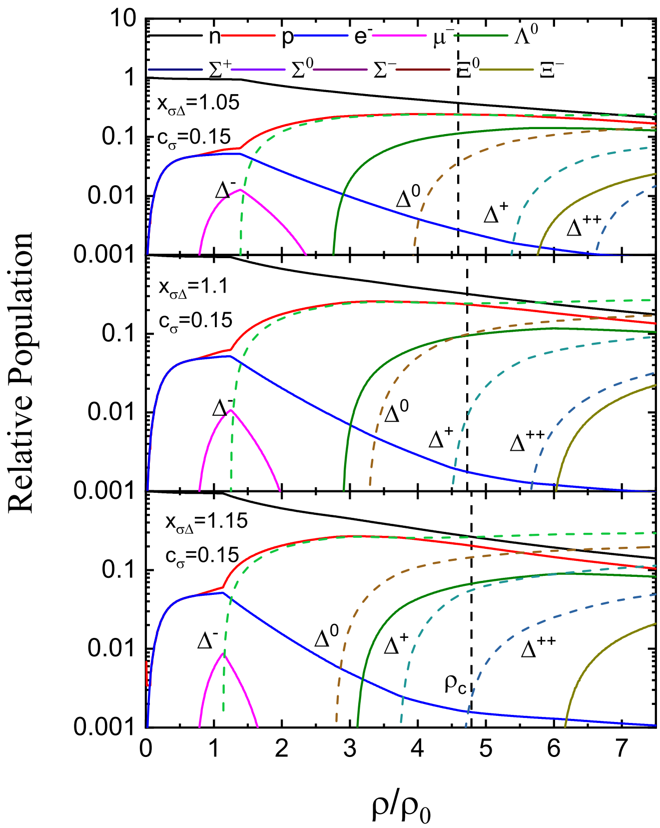

FIG. 5. Relative population of particles versus baryon density with σ-cut scheme ($c_\sigma = 0.15$), $x_{\sigma\Delta} = 1.05$, $x_{\sigma\Delta} = 1.1$, $x_{\sigma\Delta} = 1.15$, and K^- potential depth of $U_K = -160$ MeV; dashed lines denote K^- and Δ resonance.

at $6.14\rho_0$, while the critical densities of K^- meson occu at $6.79\rho_0$ and $6.73\rho_0$, respectively.

Next we examine the effect of the σ-cut scheme on the particle population. This is plotted in the Fig. 5. From Fig. 3, we determined that no K^- is generated when using the σ-cut scheme, as there is no intersection between ω_K and μ_e, but the Δ resonance has some interesting variations. The K^- disappear, and with z the decrease of μ^- the Δ^+ and Δ^{++} increase as the charge balance conditions lead to the appearance of new hyperons Ξ^-, suggesting that hyperons are more favorable as neutralizers of positive charges compared to leptons. As $x_{\sigma\Delta}$ increases from 1.05 to 1.15, the critical value of Δ resonance shifts to lower density and the central energy density (ρ_c) will move towards the high density area; in particular, when $x_{\sigma\Delta} =$ 1.15, the critical density of Δ^0 moves before that of Λ^0. From these figures, it can be concluded that the appearance of kaon meson condensation is more likely to suppress the hyperon production than the Δ resonance. Although the σ-cut scheme leads to the disappearance of kaon meson condensation, it does not change the relationship between the Δ resonance as $x_{\sigma\Delta}$ varies.

TABLE V. Threshold densities n_{cr} (in units of ρ/ρ_0) for kaon condensation in dense nuclear matter for different values of K^- optical potential depths U_K (in units of MeV) without σ-cut scheme.

	$n_{cr}(K^-)$		
U_K (MeV)	$x_{\sigma\Delta} = 1.05$	$x_{\sigma\Delta} = 1.1$	$x_{\sigma\Delta} = 1.15$
−120	none	none	none
−140	none	none	none
−160	5.24	6.79	6.73

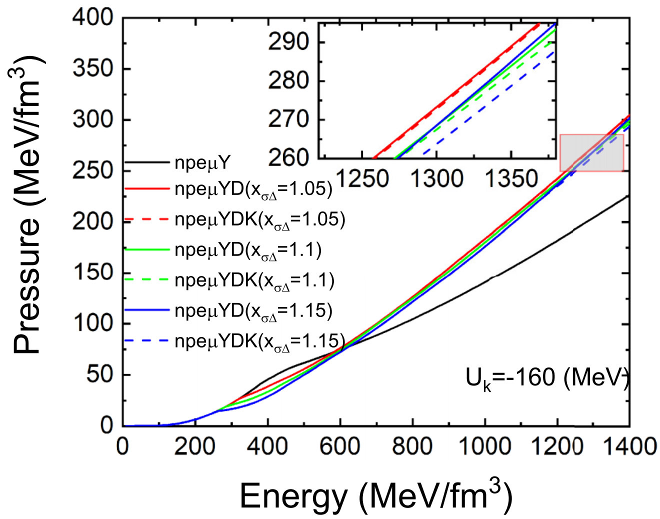

FIG. 6. Pressure versus energy density without the σ-cut scheme. The solid line is for n, p, leptons, and hyperons whereas others are with additional Δ resonance; dashed lines denote K^- mesons and exhibit $U_K = -160$ MeV.

Next we can discuss some properties of the neutron star. Figure 6 shows pressure as a function of energy density in NS matter containing Δ resonance and K^- without the σ-cut scheme. We can see from the enlarged area in the figure that the addition of K^- softens the equation of state to some extent, although this is not particularly significant with the onset of

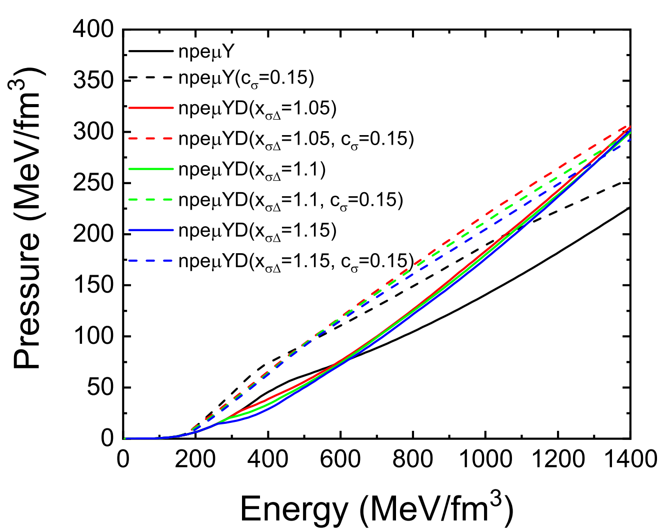

FIG. 7. Pressure versus energy density with σ-cut scheme. The solid line is for n, p, leptons, and hyperons whereas others are with additional Δ resonance; the dashed line exhibits $c_\sigma = 0.15$.

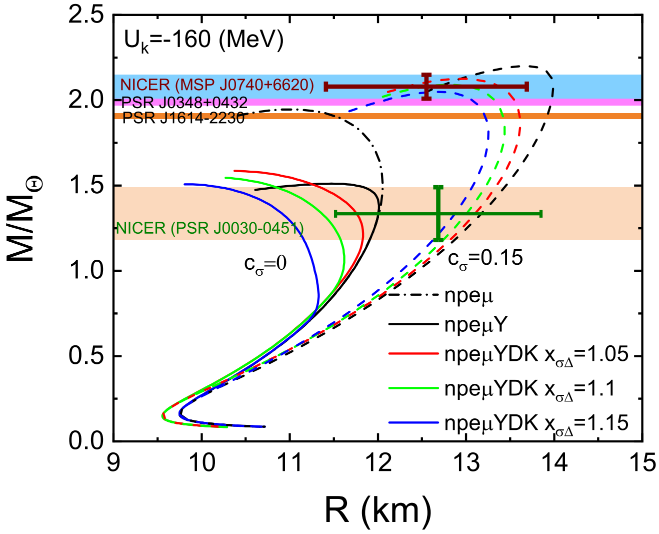

FIG. 8. Mass-radius relation using and not using σ-cut scheme in NS matter including hyperons, Δ resonance, and K^-. The solid lines denote results without σ-cut; dashed lines denote $c_\sigma = 0.15$. The horizontal bars indicate the observational constraints of PSR J1614−2230 [1–4], PSR J0348+0432 [5], MSP J0740+6620 [6], and PSR J0030−0451 [68].

the Δ resonance. As $x_{\omega\Delta}$ increases, the EOS will get softer, eventually leading to a decrease in the maximum mass of the neutron star. It is worth mentioning that Δ resonance softens the EOS when the energy density is between 300 and 600 MeV/fm^3 and stiffens significantly >600 MeV/fm^3 compared to the case where only hyperons are included, and intensifies with increasing $x_{\sigma\Delta}$ (1.05 → 1.15), which suggests the existence of a softer EOS in the low-density region, and the recent constraints on tidal deformation and radius point to this. When the σ-cut scheme is considered, we plot the EOS in Fig. 7. From Fig. 3 we determined that there is no K^- when using σ-cut scheme, so the composition contains only hyperons and Δ. We can see that σ-cut scheme significantly stiffens the EOS, and it is the truncated intensity of σ meson field strength in Fig. 1 that leads to this result, and still retains the EOS softening feature in the low density region. The EOS obtained by this way can generate a heavier $2M_\odot$ NS by solving the Tolman-Oppenheimer-Volkoff (TOV) equation, in order to eliminate the "hyperon puzzle."

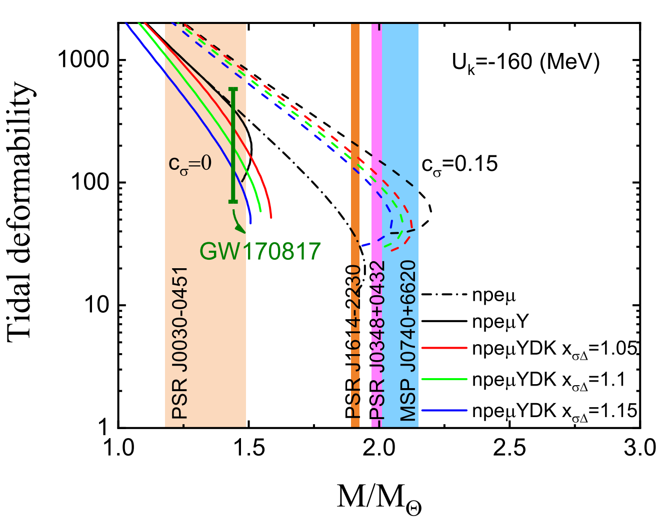

FIG. 9. The dimensionless tidal deformability as a function of star mass. The solid line indicates without σ-cut scheme; the dashed line indicates $c_\sigma = 0.15$. The constraints from the GW170817 event for tidal deformability are shown.

The results of the mass-radius relation for a NS is discussed here and shown in Fig. 8. The constraints from the observables of massive neutron stars, PSR J1614−2230 [1–4] and PSR J034+0432 [5] are also shown as the shaded bands. The Neutron star Interior Composition Explorer (NICER) Collaboration reported an accurate measurement of mass and radius of PSR J0030+0451 [68] in 2019, and MSP J0740+6620 in 2021 [6]. For the solid lines without σ-cut, different coupling parameters $x_{\sigma\Delta}$ have a significant effect on the maximum mass and radius of a NS; it shows that the Δ resonance increases the maximum mass of the NS and decreases the radius. With the increase of $x_{\sigma\Delta}$ (1.05 → 1.15), the maximum mass decreases, but is still greater than in the case of pure hyperons. The dashed lines denote $c_\sigma = 0.15$; this scheme can significantly increase the maximum mass of the neutron star and make it heavier than $2M_\odot$, and also accords with the constraints from gravitational waves and NICER (MSP J0740+6620). Note that there is no appearance of K^- when $c_\sigma = 0.15$ from Fig. 3. We list the simultaneous measurement of radius for MSP J0740+6620 and PSR J0030−0451 from the NICER data and maximum mass of the neutron star for various values of $x_{\sigma\Delta}$ in Table VI. The tidal deformability Λ, as a function of neutron star mass is shown in Fig. 9. From the gravitational wave of the binary NS merger GW170817, it was extracted as $\Lambda_{1.4} = 190^{+390}_{-120}$ at $1.4M_\odot$ [69]. From the figure we can see that the σ-cut scheme with the stiffer EOS has the larger $\Lambda_{1.4}$ and heavier masses, whose $\Lambda_{1.4}$ are beyond the constraint of GW170817, while the softer EOS satisfies the constraints of GW170817 and has smaller radii without the σ-cut scheme, and the Λ is still within the bound of GW170817 after considering the Δ resonance. With the strong constraint on the compositions of compact stars by the observational tidal deformability, we think it is necessary to consider Δ resonance in the softer EOS in the event GW170817, as well as the tidal deformability of the neutron star at $2.0M_\odot$, which is expected to be measured in future gravitational wave events from binary neutron-star mergers.

IV. SUMMARY

In this paper, we have discussed the Δ resonance and kaon meson condensation inside a neutron star under the IUFSU model, using to the recent rapid results of astronomical observations on the radii and tidal deformations of compact stars. However, the maximum masses of neutron stars generated by the softer EOS (hyperon puzzle) cannot approach $2.0M_\odot$, as it did not satisfy the constraints from the massive neutron star observables, so we used the σ-cut scheme and got the maximum mass heavier than $2M_\odot$.

TABLE VI. The maximum mass (in units of solar mass $M_{\odot}$) and radius (km) in NS matter including hyperons, Δ resonance, and K^- using and not using σ-cut scheme with potential $U_K = -160$ MeV.

	Without σ-cut			$c_\sigma = 0.15$			MSP J0740 + 6620 [6]		PSR J0030 − 0451 [8]	
	M	ρ_c	R	M	ρ_c	R	M	R	M	R
(n, p)	1.93	1.029	11.14							
(n, p, Y)	1.51	0.87	11.47	2.2	0.58	13.65	2.08 ± 0.07	$12.39^{+1.3}_{-0.98}$	$1.34^{+0.15}_{-0.16}$	$12.71^{+1.14}_{-1.19}$
$x_{\sigma\Delta} = 1.05$ $(n, p, Y, D, (K^-))$	1.58	1.24	10.37	2.12	0.71	12.93				
$x_{\sigma\Delta} = 1.1$ $(n, p, Y, D, (K^-))$	1.54	1.3	10.27	2.09	0.73	12.84				
$x_{\sigma\Delta} = 1.15$ $(n, p, Y, D, (K^-))$	1.51	1.37	9.9	2.05	0.74	12.64				

We find that the kaon condensation cannot appear in the hyperons and Δ resonance with our parameter $U_K = -120$ and -140 MeV; it occurs only at $U_K = -160$ MeV, and the Δ resonance also shifts the kaon meson toward the high-density region. In NS matter containing hyperons and Δ resonances, the effect of the kaon meson on EOS is very insignificant.

On the other hand, we investigated the effect of $x_{\sigma\Delta}$ on the Δ resonance; for the Δ coupling constants, we take $x_{\sigma\Delta} =$ 1.05, 1.1, and 1.15, and the value of $x_{\sigma\Delta}$ has great influence on the relative population of particles as a function of the baryon density. We find that the inclusion of Δ resonance shifts the critical density of hyperons towards the high density region from $x_{\sigma\Delta} = 1.05$ to $x_{\sigma\Delta} = 1.15$ and the critical density of Δ resonance will move toward the low density region. Also, the EOS softens as $x_{\sigma\Delta}$ increases.

When the σ-cut scheme is not used, we find that the softer EOS considering Δ resonance is still within the $\Lambda_{1.4}$ range of GW170817, and this may suggest the existence of a softer EOS in the low-density region, while the softer EOS satisfies the constraints of GW170817 and has smaller radii. When we used the σ-cut scheme and take the parameter $c_\sigma = 0.15$, we find that the maximum mass and radius of NSs obtained under this model are close to the NICER (MSP J0740+6620) constraint. For tidal deformability of neutron stars with maximum mass above $2M_{\odot}$, future gravitational wave events of binary neutron star mergers may provide new constraints.

[1] P. Demorest, T. Pennucci, S. Ransom, M. Roberts, and J. Hessels, Shapiro delay measurement of a two solar mass neutron star, Nature (London) **467**, 1081 (2010).

[2] Z. Arzoumanian *et al.*, The NANOGrav 11-year data set: High-precision timing of 45 millisecond pulsars, Astrophys. J. Suppl. **235**, 37 (2018).

[3] E. Fonseca *et al.*, The NANOGrav nine-year data set: Mass and geometric measurements of binary millisecond pulsars, Astrophys. J. **832**, 167 (2016).

[4] F. Ozel, D. Psaltis, S. Ransom, P. Demorest, and M. Alford, The massive pulsar PSR J1614-2230: Linking quantum chromodynamics, gamma-ray bursts, and gravitational wave astronomy, Astrophys. J. Lett. **724**, L199 (2010).

[5] J. Antoniadis, P. C. C. Freire, N. Wex, T. M. Tauris, R. S. Lynch, M. H. Van Kerkwijk, M. Kramer, C. Bassa, V. S. Dhillon, T. Driebe *et al.*, A massive pulsar in a compact relativistic binary, Science **340**, 1233232 (2013).

[6] E. Fonseca, H. T. Cromartie, T. T. Pennucci, P. S. Ray, A. Y. Kirichenko, S. M. Ransom, P. B. Demorest, I. H. Stairs, Z. Arzoumanian, L. Guillemot *et al.*, Refined mass and geometric measurements of the high-mass PSR J0740 + 6620, Astrophys. J. Lett. **915**, L12 (2021).

[7] H. T. Cromartie *et al.*, Relativistic Shapiro delay measurements of an extremely massive millisecond pulsar, Nat. Astron. **4**, 72 (2019).

[8] T. E. Riley, A. L. Watts, P. S. Ray, S. Bogdanov, S. Guillot, S. M. Morsink, A. V. Bilous, Z. Arzoumanian, D. Choudhury, J. S. Deneva *et al.*, A NICER view of the massive pulsar PSR J0740 + 6620 informed by radio timing and XMM-Newton spectroscopy, Astrophys. J. Lett. **918**, L27 (2021).

[9] B. P. Abbott *et al.*, Properties of the Binary Neutron Star Merger GW170817, Phys. Rev. X **9**, 011001 (2019).

[10] M. W. Coughlin *et al.*, Constraints on the neutron star equation of state from AT2017gfo using radiative transfer simulations, Mon. Not. R. Astron. Soc. **480**, 3871 (2018).

[11] J. Schaffner and I. N. Mishustin, Hyperon rich matter in neutron stars, Phys. Rev. C **53**, 1416 (1996).

[12] C. Wu and Z. Ren, Strange hadronic stars in relativistic mean-field theory with the FSUGold parameter set, Phys. Rev. C **83**, 025805 (2011).

[13] T.-T. Sun, S.-S. Zhang, Q.-L. Zhang, and C.-J. Xia, Strangeness and Δ resonance in compact stars with relativistic-mean-field models, Phys. Rev. D **99**, 023004 (2019).

[14] K. A. Maslov, E. E. Kolomeitsev, and D. N. Voskresensky, Δ resonances and charged ρ mesons in neutron stars, J. Phys.: Conf. Ser. **932**, 012040 (2017).

[15] E. E. Kolomeitsev, K. A. Maslov, and D. N. Voskresensky, Delta isobars in relativistic mean-field models with σ-scaled hadron masses and couplings, Nucl. Phys. A **961**, 106 (2017).

[16] A. Sedrakian and A. Harutyunyan, Delta-resonances and hyperons in proto-neutron stars and merger remnants, Eur. Phys. J. A **58**, 137 (2022).

[17] A. Drago, A. Lavagno, G. Pagliara, and D. Pigato, Early appearance of Δ isobars in neutron stars, Phys. Rev. C **90**, 065809 (2014).

[18] N. K. Glendenning, Neutron stars are giant hypernuclei? Astrophys. J. **293**, 470 (1985).

[19] V. Dexheimer, K. D. Marquez, and D. P. Menezes, Delta baryons in neutron-star matter under strong magnetic fields, Eur. Phys. J. A **57**, 216 (2021).

[20] K. D. Marquez, M. R. Pelicer, S. Ghosh, J. Peterson, D. Chatterjee, V. Dexheimer, and D. P. Menezes, Exploring the effects of Δ baryons in magnetars, Phys. Rev. C **106**, 035801 (2022).

[21] T. Schürhoff, S. Schramm, and V. Dexheimer, Neutron stars with small radii—the role of Δ resonances, Astrophys. J. Lett. **724**, L74 (2010).

[22] V. B. Thapa and M. Sinha, Dense matter equation of state of a massive neutron star with antikaon condensation, Phys. Rev. D **102**, 123007 (2020).

[23] T. Maruyama, T. Tatsumi, D. N. Voskresensky, T. Tanigawa, T. Endo, and S. Chiba, Finite size effects on kaonic pasta structures, Phys. Rev. C **73**, 035802 (2006).

[24] G. E. Brown, C.-H. Lee, H.-J. Park, and M. Rho, Strangeness Condensation by Expanding about the Fixed Point of the Harada-Yamawaki Vector Manifestation, Phys. Rev. Lett. **96**, 062303 (2006).

[25] G.-y. Shao and Y.-x. Liu, Influence of the isovector-scalar channel interaction on neutron star matter with hyperons and antikaon condensation, Phys. Rev. C **82**, 055801 (2010).

[26] P. Char and S. Banik, Massive neutron stars with antikaon condensates in a density dependent hadron field theory, Phys. Rev. C **90**, 015801 (2014).

[27] G. F. Burgio, H. J. Schulze, I. Vidana, and J. B. Wei, Neutron stars and the nuclear equation of state, Prog. Part. Nucl. Phys. **120**, 103879 (2021).

[28] D. Logoteta, Hyperons in neutron stars, Universe **7**, 408 (2021).

[29] G. F. Burgio, H.-J. Schulze, and A. Li, Hyperon stars at finite temperature in the Brueckner theory, Phys. Rev. C **83**, 025804 (2011).

[30] D. Lonardoni, A. Lovato, S. Gandolfi, and F. Pederiva, Hyperon Puzzle: Hints from Quantum Monte Carlo Calculations, Phys. Rev. Lett. **114**, 092301 (2015).

[31] I. Bombaci, The hyperon puzzle in neutron stars, JPS Conf. Proc. **17**, 101002 (2017).

[32] L. Bonanno and A. Sedrakian, Composition and stability of hybrid stars with hyperons and quark color-superconductivity, Astron. Astrophys. **539**, A16 (2012).

[33] G. Colucci and A. Sedrakian, Equation of state of hypernuclear matter: Impact of hyperon–scalar-meson couplings, Phys. Rev. C **87**, 055806 (2013).

[34] M. Fortin, C. Providencia, A. R. Raduta, F. Gulminelli, J. L Zdunik, P. Haensel, and M. Bejger, Neutron star radii and crusts: Uncertainties and unified equations of state, Phys. Rev. C **94**, 035804 (2016).

[35] Y. Chen, H. Guo, and Y. Liu, Neutrino scattering rates in neutron star matter with Δ isobars, Phys. Rev. C **75**, 035806 (2007).

[36] J. J. Li, A. Sedrakian, and M. Alford, Relativistic hybrid stars with sequential first-order phase transitions and heavy-baryon envelopes, Phys. Rev. D **101**, 063022 (2020).

[37] J. J. Li and A. Sedrakian, Implications from GW170817 for δ-isobar admixed hypernuclear compact stars, Astrophys. J. Lett. **874**, L22 (2019).

[38] Z.-Y. Zhu, E.-P. Zhou, and A. Li, Neutron star equation of state from the quark level in light of GW170817, Astrophys. J. **862**, 98 (2018).

[39] T. Malik, N. Alam, M. Fortin, C. Providência, B. K. Agrawal, T. K. Jha, Bharat Kumar, and S. K. Patra, GW170817: Constraining the nuclear matter equation of state from the neutron star tidal deformability, Phys. Rev. C **98**, 035804 (2018).

[40] N. K. Glendenning and S. A. Moszkowski, Reconciliation of Neutron Star Masses and Binding of the Λ in Hypernuclei, Phys. Rev. Lett. **67**, 2414 (1991).

[41] J. J. Li, A. Sedrakian, and F. Weber, Competition between delta isobars and hyperons and properties of compact stars, Phys. Lett. B **783**, 234 (2018).

[42] P. Ribes, A. Ramos, L. Tolos, C. Gonzalez-Boquera, and M. Centelles, Interplay between Δ particles and hyperons in neutron stars, Astrophys. J. **883**, 168 (2019).

[43] N. K. Glendenning and J. Schaffner-Bielich, First order kaon condensate, Phys. Rev. C **60**, 025803 (1999).

[44] N. K. Glendenning and J. Schaffner-Bielich, Kaon Condensation and Dynamical Nucleons in Neutron Stars, Phys. Rev. Lett. **81**, 4564 (1998).

[45] D. B. Kaplan and A. E. Nelson, Strange goings on in dense nucleonic matter, Phys. Lett. B **175**, 57 (1986).

[46] A. E. Nelson and D. B. Kaplan, Strange condensate realignment in relativistic heavy ion collisions, Phys. Lett. B **192**, 193 (1987).

[47] K. A. Maslov, E. E. Kolomeitsev, and D. N. Voskresensky, Making a soft relativistic mean-field equation of state stiffer at high density, Phys. Rev. C **92**, 052801(R) (2015).

[48] F. Ma, W. Guo, and C. Wu, Kaon meson condensate in neutron star matter including hyperons, Phys. Rev. C **105**, 015807 (2022).

[49] F. Wu and C. Wu, Hyperonized neutron stars within the framework of the σ-cut scheme, Eur. Phys. J. A **56**, 20 (2020).

[50] F. J. Fattoyev, C. J. Horowitz, J. Piekarewicz, and G. Shen, Relativistic effective interaction for nuclei, giant resonances, and neutron stars, Phys. Rev. C **82**, 055803 (2010).

[51] F. Grill, H. Pais, C. Providência, I. Vidaña, and S. S. Avancini, Equation of state and thickness of the inner crust of neutron stars, Phys. Rev. C **90**, 045803 (2014).

[52] J. Schaffner, C. B. Dover, A. Gal, C. Greiner, D. J. Millener, and H. Stoecker, Multiply strange nuclear systems, Ann. Phys. **235**, 35 (1994).

[53] J. Hu, Y. Zhang, and H. Shen, The Ξ-nuclear potential constrained by recent Ξ^- hypernuclei experiments, J. Phys. G **49**, 025104 (2022).

[54] M. Fortin, S. S. Avancini, C. Providência, and I. Vidaña, Hypernuclei and massive neutron stars, Phys. Rev. C **95**, 065803 (2017).

[55] P. Khaustov *et al.*, Evidence of Ξ hypernuclear production in the $^{12}\mathrm{C}(K^-, K^+)^{12}_{\Xi}\mathrm{Be}$ reaction, Phys. Rev. C **61**, 054603 (2000).

[56] S. Banik and D. Bandyopadhyay, A Third family of superdense stars in the presence of anti-kaon condensates, Phys. Rev. C **64**, 055805 (2001).

[57] Z.-X. Li, G.-J. Mao, Y.-Z. Zhuo, and W. Greiner, Transition to Δ matter from hot, dense nuclear matter within a relativistic mean field formulation of the nonlinear σ and ω model, Phys. Rev. C **56**, 1570 (1997).

[58] X.-m. Jin, QCD sum rules for delta isobar in nuclear matter, Phys. Rev. C **51**, 2260 (1995).

[59] D. S. Kosov, C. Fuchs, B. V. Martemyanov, and A. Faessler, Constraints on the relativistic mean field of Δ-isobar in nuclear matter, Phys. Lett. B **421**, 37 (1998).

[60] A. Drago, A. Lavagno, and G. Pagliara, Can very compact and very massive neutron stars both exist? Phys. Rev. D **89**, 043014 (2014).

[61] V. B. Thapa, M. Sinha, J. J. Li, and A. Sedrakian, Massive Δ-resonance admixed hypernuclear stars with antikaon condensations, Phys. Rev. D **103**, 063004 (2021).

[62] M. Baldo, I. Bombaci, and G. F. Burgio, Microscopic nuclear equation of state with three-body forces and neutron star structure, Astron. Astrophys. **328**, 274 (1997).

[63] T. Hinderer, Tidal Love numbers of neutron stars, Astrophys. J. **677**, 1216 (2008).

[64] S. Postnikov, M. Prakash, and J. M. Lattimer, Tidal love numbers of neutron and self-bound quark stars, Phys. Rev. D **82**, 024016 (2010).

[65] T. Hinderer, B. D. Lackey, R. N. Lang, and J. S. Read, Tidal deformability of neutron stars with realistic equations of state and their gravitational wave signatures in binary inspiral, Phys. Rev. D **81**, 123016 (2010).

[66] Y.-H. Song, R. Lazauskas, and V. Gudkov, Time reversal invariance violating and parity conserving effects in neutron deuteron scattering, Phys. Rev. C **84**, 025501 (2011); **93**, 049901(E) (2016).

[67] E. E. Kolomeitsev, K. A. Maslov, and D. N. Voskresensky, Hyperon puzzle and the RMF model with scaled hadron masses and coupling constants, J. Phys.: Conf. Ser. **668**, 012064 (2016).

[68] T. E. Riley, A. L. Watts, S. Bogdanov, P. S. Ray, R. M. Ludlam, S. Guillot, Z. Arzoumanian, C. L. Baker, A. V. Bilous, D. Chakrabarty *et al.*, A NICER view of PSR j0030 + 0451: Millisecond pulsar parameter estimation, Astrophys. J. Lett. **887**, L21 (2019).

[69] B. P. Abbott *et al.*, GW170817: Measurements of Neutron Star Radii and Equation of State, Phys. Rev. Lett. **121**, 161101 (2018).